Numerical Simulation of Magnetic Field and Flow Control in Mold with Vertical Combination Electromagnetic Brake

F. Li, E. Wang, M. Feng

VC-EMBr (vertical combination electromagnetic Brake) technology which V-EMBr (vertical electromagnetic brake)is combined with EMBr-Ruler is proposed, and it is intended to control impact of the molten steel jet on narrow face while strengthening control of impacted depth in lower circulation zone. Features of magnetic field, flow field and trajectories of inclusion particles in mold with VC-EMBr are researched by numerical simulation method. The results show that the effective magnetic field induced by VC-EMBr not only covers the entire mold width, but also covers free surface near narrow face and solidified shell frontier area where is impacted firstly by the molten steel jet from SEN (submerged entry nozzle). The steady DC magnetic field of VC-EMBr can weaken molten steel flow in mold and inhibit velocity of the molten steel jet and its impacted strength on narrow face, the impacted depth in lower circulation is reduced drastically, the molten steel velocity of free surface is reduced, the divergent degree of velocity distribution of impacted point and its surrounding area of narrow face is reduced significantly and the removal efficiency of inclusion particles is improved. Therefore, VC-EMBr can reduce slag, prevent leakage and promote inclusion particles floating and separating effectively, which help to improve the slab purity. The significant metallurgical effect characterized by numerical simulation results accord the design intention, lay the foundation for experimental research and also provide preliminary theory for research and development of VC-EMBr.

KEYWORDS: ELECTROMAGNETIC BRAKE - MAGNETIC FIELD - FLOW FIELD - INCLUSION MOVEMENT - CONTINUOUS CASTING

INTRODUCTION

In the early 1980s, EMBr (electromagnetic brake) technology was presented in order to improve the purity of finished slab in continuous casting process, after years of research and practice, EMBr technology has become a relatively mature electromagnetic technology currently, by controlling the molten metal flow can control the ingredient distribution of slab, and the effects can achieve to reduce slag, prevent leakage of steel, stabilize surface fluctuations and promote nonmetallic inclusion particles floating and separating, so the quality of slab is improved effectively with EMBr [1-3]. In view of the notable characteristics of EMBr, the application and research of EMBr technology have been extensively developed in recent years [4-11].

Controlling the narrow face area of mold where is impacted by the molten steel jet from SEN (submerged entry nozzle) is the key factor to control surface fluctuations, slag, leakage and float and separation of inclusion particles. The magnetic pole of V-EMBr (vertical electromagnetic brake) is placed vertically near narrow face and along the height direction of mold, which is different from horizontal arrangement of magnetic pole of traditional EMBr device, the simulation results reveal that the flow control effect of V-EMBr is effective in mold and the metallurgical effect is satisfied [12]. On the basis of V-EMBr, VC-EMBr (vertical combination electromagnetic brake) technology which V-EMBr is combined with EMBr-Ruler is put forward, the schematic diagram of the device is shown in Fig.1. The added magnetic pole is placed vertically and near narrow face on the original magnetic pole of EMBr-Ruler, the remaining structure of VC-EMBr is same as EMBr-Ruler, the original magnetic pole is called main magnetic

Fei Li, Engang Wang, Mingjie Feng
Key Laboratory of Electromagnetic Processing of Materials,
Northeastern University, NO. 3-11,
Wenhua Road, Heping District, Shenyang, P. R. China.

Engang Wang (Corresponding author)
zkp198563@sina.com

pole and the vertical one is called minor magnetic pole. VC-EMBr is intended to control impact of the molten steel jet from SEN on narrow face while strengthening control of impacted depth in lower circulation zone. The magnetic field and flow field in mold with VC-EMBr are calculated by simulation method, and the effect of metallurgy is studied, which lay the groundwork for the experimental research and provide the preliminary theory for study and development of VC-EMBr.

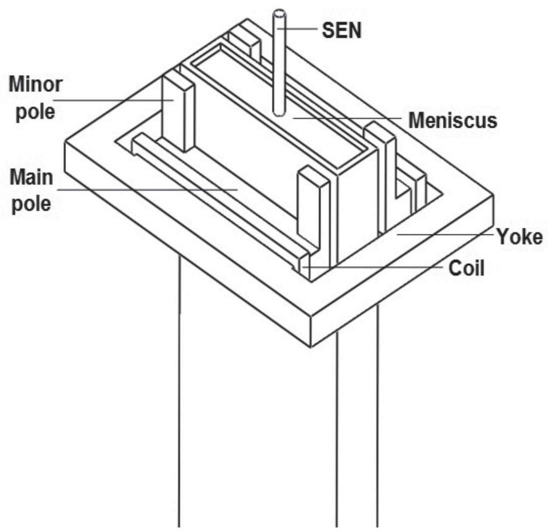

Fig. 1 - Schematic diagram of VC-EMBr device

ESTABLISHMENT OF MATHEMATICAL MODEL

Governing Equations of Magnetic Field

The molten steel flow in mold with EMBr is a steady state. The effect of the slow molten steel flow on distribution of magnetic field is ignored, and the volume density of the free charge is also ignored. The electromagnetic properties of molten steel are considered to be uniform and isotropic. The electric potential equation is solved to get the current density [13].

The equation of induced current density J

$$J=\sigma(-\nabla\phi+U\times B) \tag{1}$$

The electric field intensity is represented by electric potential ϕ

$$E=-\nabla\phi \tag{2}$$

The continuity equation of induced current density J

$$\nabla\cdot J=0 \tag{3}$$

The equation of electric potential ϕ is derived by (1) and (3)

$$\nabla^2\phi=\nabla\cdot(U\times B) \tag{4}$$

The equation of electromagnetic force F_m

$$F_m=J\times B \tag{5}$$

Where J is the induced current density, A/m^2, σ is the conductivity of the liquid steel, S/m, ϕ is the electric potential, V, U is the flow velocity of molten steel, m/s, B is the magnetic flux density, T, E is the electric field strength, V/m, F_m is the electromagnetic force, N/m^3.

Governing Equations of Flow Field

The three-dimensional flow field in mold with EMBr is calculated by some assumptions as follows. The interface between molten steel and mold is no-slip boundary, and the flow velocity of molten steel at the wall is zero. The flow of molten steel is single-phase flow, and physical parameters are constant. The impact of mold taper, solidified strand shell and vibration on molten steel flow are ignored. The liquid surface of molten steel is flat, the impact of mold powder is not considered. The governing equations of three-dimensional flow field in mold are shown below.

The continuity equation

$$\frac{\partial(\rho_s u_j)}{\partial x_j}=0 \tag{6}$$

The momentum equation

$$\rho_s\frac{\partial u_i}{\partial t}+\rho_s\frac{\partial(u_i u_j)}{\partial x_j}=-\frac{\partial P}{\partial x_i}+\frac{\partial}{\partial x_i}(\mu_{eff}\frac{\partial u_j}{\partial x_i})+\frac{\partial}{\partial x_j}(\mu_{eff}\frac{\partial u_i}{\partial x_j})+\rho_s g_i+F_m \tag{7}$$

k – ε equations [14]

k equation

$$\rho_s\frac{\partial(ku_i)}{\partial x_i}=\frac{\partial}{\partial x_i}[(\mu+\frac{|f_\mu|\mu_t}{\sigma_k})\frac{\partial k}{\partial x_i}]+G_k-\rho_s\varepsilon-\left|2\mu(\frac{\partial k^{1/2}}{\partial n})^2\right| \tag{8}$$

ε equation

$$\rho_s\frac{\partial(\varepsilon u_i)}{\partial x_i}=\frac{\partial}{\partial x_i}[(\mu+\frac{|f_\mu|\mu_t}{\sigma_\varepsilon})\frac{\partial\varepsilon}{\partial x_j}]+\frac{C_{1\varepsilon}\varepsilon}{k}G_k|f_1|-C_{2\varepsilon}\rho_s\frac{\varepsilon^2}{k}|f_2|+\left|2\frac{\mu|f_\mu|\mu_t}{\rho}(\frac{\partial^2 u}{\partial n^2})^2\right| \tag{9}$$

$$\mu_{eff}=\mu_1+\mu_t \tag{10}$$

$$\mu_t=C_\mu|f_\mu|\rho_s\frac{k^2}{\varepsilon} \tag{11}$$

Where u_i, u_j is the component of flow velocity in the x_i, x_j direction, m/s, ρ_s is the density of molten steel, kg/m^3, P is the pressure of molten steel, Pa, μ_{eff} is the effective viscosity coefficient, kg/(m·s), μ_1 is the viscosity coefficient of molecular, kg/(m·s), μ_t is the viscosity coefficient of turbulent, kg/(m·s), g_i is the volume force of i direction, m/s^2, μ is the dynamic viscosity of molten steel, kg/(m·s), k is the kinetic energy of turbulent fluctuation, m^2/s^2, G_k is the growth rate of turbulent kinetic energy k, ε is the dissipation rate of turbulent kinetic energy, m^2/s^3, coefficient $C_{1\varepsilon}$, $C_{2\varepsilon}$, C_μ, σ_ε and σ_k are 1.44, 1.92, 0.09, 1.3 and 1.0 [15], coefficient f_1, f_2 and f_μ are the revision of the standard Reynolds equation $C_{1\varepsilon}$, $C_{2\varepsilon}$ and C_μ.

Governing Equations of Movement of Inclusion Particles

Calculating the movement of the inclusion particle in mold is on the following assumptions [16]. Since the flow is steady, so the average time result of movement of inclusion particle is not considered changing with time and the length of time. The inclusion particle is considered to be a small sphere, and its movement is with the flow and without considering the impact and role on the flow field. The behaviors of polymerization, growth, collision and fragmentation are not considered, the size of the inclusion particle remains constant. When the inclusion particle moves to be captured at the free surface, it is thought to be removed. The governing equations of movement of the inclusion particle in mold are as follows.

$$\frac{du_p}{dt} = F_D(U - u_p) + \frac{g_i(\rho_p - \rho_s)}{\rho_p} + F_i \qquad (12)$$

Where, $F_D(U-u_p)$ is the drag force of unit mass of the inclusion particle.

$$F_D = \frac{18\mu}{\rho_p d_p^2}\frac{C_D R_e}{24} \qquad (13)$$

Where, u_p is velocity of the inclusion particle, m/s; ρ_p is the density of the inclusion particle, kg/m^3; d_p is the diameter of the inclusion particle, m; F_i is the additional force of the inclusion particle, N/kg; C_D is the drag coefficient, and it is a function of the relative Reynolds (Re). Re is expressed as follow.

$$R_e = \frac{\rho d_p \left|u_p - U\right|}{\mu} \qquad (14)$$

Boundary Conditions

Since the slab is with symmetry, the whole and quarter volume of the slab is taken to calculate magnetic field and flow field respectively. The boundary conditions are set as follows.

(1) The components of velocity and current density which are perpendicular to the wall are zero, and the components which are parallel to the mold wall are used no-slip boundary condition.
(2) The gradient of each variable on free surface of molten steel is zero along the normal direction.
(3) The gradient of each variable on symmetry plane is zero along the normal direction.
(4) The inlet is defined as the inlet of SEN, the inlet velocity is determined according to the casting speed, $K_{inlet}=0.01U_{inlet}^2$, $\varepsilon_{inlet}=K_{inlet}^{3/2}(d_0/2)$, U_{inlet} is the inlet velocity, d_0 is the inlet diameter.
(5) The outlet is defined as the bottom of the computational domain, and the normal derivative of each variable is zero along this section.
(6) When calculating the trajectories of inclusion particles, boundary condition of wall and symmetry plane are set to reflect, that of inlet and outlet are set to escape and that of free surface is set to trap.

The mainly parameters for calculating which are provided by a domestic steel mill are shown in Table 1.

Tab.1 - Parameters of numerical simulation

Parameter	Value
Mold width, mm	1450
Mold thickness, mm	230
Molten steel density, kg/m^3	7020
Molten steel viscosity, Pa·s	6.2×10^{-3}
Molten steel electric conductivity, S/m	7.14×10^{5}
Electric current, A	850
Casting speed, m/min	1.6
Submerged depth of SEN, mm	170
Outlet angle of SEN, deg	-15

Solving Method

The calculation is divided into two steps. First, the three-dimensional model of magnetic field in mold with VC-EMBr is established by ANSYS software and then it is solved to obtain the distribution of magnetic flux density. Second, the three-dimensional model of flow field in mold is established and the MHD (magneto hydrodynamics) module is called by FLUENT software, the simulated result of magnetic field in first step is the load for coupling calculation of flow field and magnetic field, and the DPM (discrete phase model) is used to solve the trajectories of inclusion particles. The SIMPLE method is adopted in this calculation, after setting the relative residuals of mass source term of continuity equation and each velocity component, the procedure begins to calculate, when the iteration is the convergence criteria 0.0001, the procedure exits automatically and then the three-dimensional distribution of flow field and the trajectories of inclusion particles in mold with VC-EMBr are obtained.

Distribution Of Magnetic Field In Mold With VC-EMBr

The distribution of magnetic flux density in mold with VC-EMBr is shown in Fig.2.

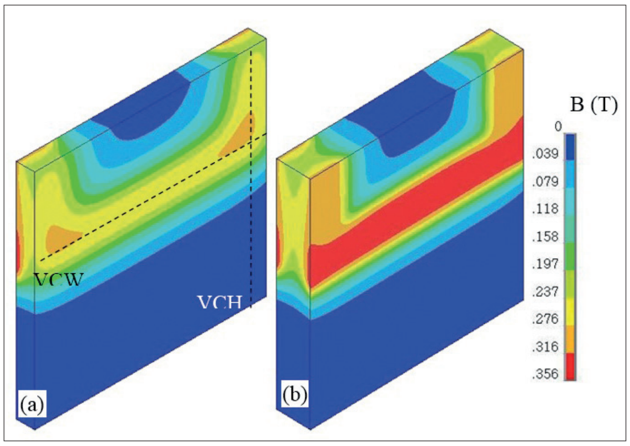

Fig. 2 - Distribution of magnetic flux density in mold with VC-EMBr

(a) — 1/2 volume, (b) — whole volume.

Fig. 2 shows that the magnetic field generated by VC-EMBr can penetrate mold copper wall and exist in molten steel, the magnetic flux density in molten steel is mainly concentrated in the covered area of main and minor magnetic pole and is decayed gradually out of the covered area. Since the coils are wound around the main magnetic pole, the magnetic flux density in the covered area of main magnetic pole is greater than that of minor magnetic pole. In the covered area of magnetic pole, the magnetic flux density is increased from slab center to slab surface along the mold thickness direction gradually, getting closer to magnetic pole is the main reason to cause the phenomenon.

In Fig. 2, the straight line VCW and VCH pass through the center point of the covered area of main and minor magnetic pole respectively. The intersected point of the two straight lines (VCW, VCH) as the middle point and along the mold thickness direction, the straight line VCT is marked and its length is equal to the mold thickness. To further understand the distribution laws of magnetic flux density in mold with VC-EMBr, the magnetic flux density on VCW, VCH and VCT are shown in Fig. 3 to analyze the change trend of magnetic flux density in molten steel of the three characteristic positions.

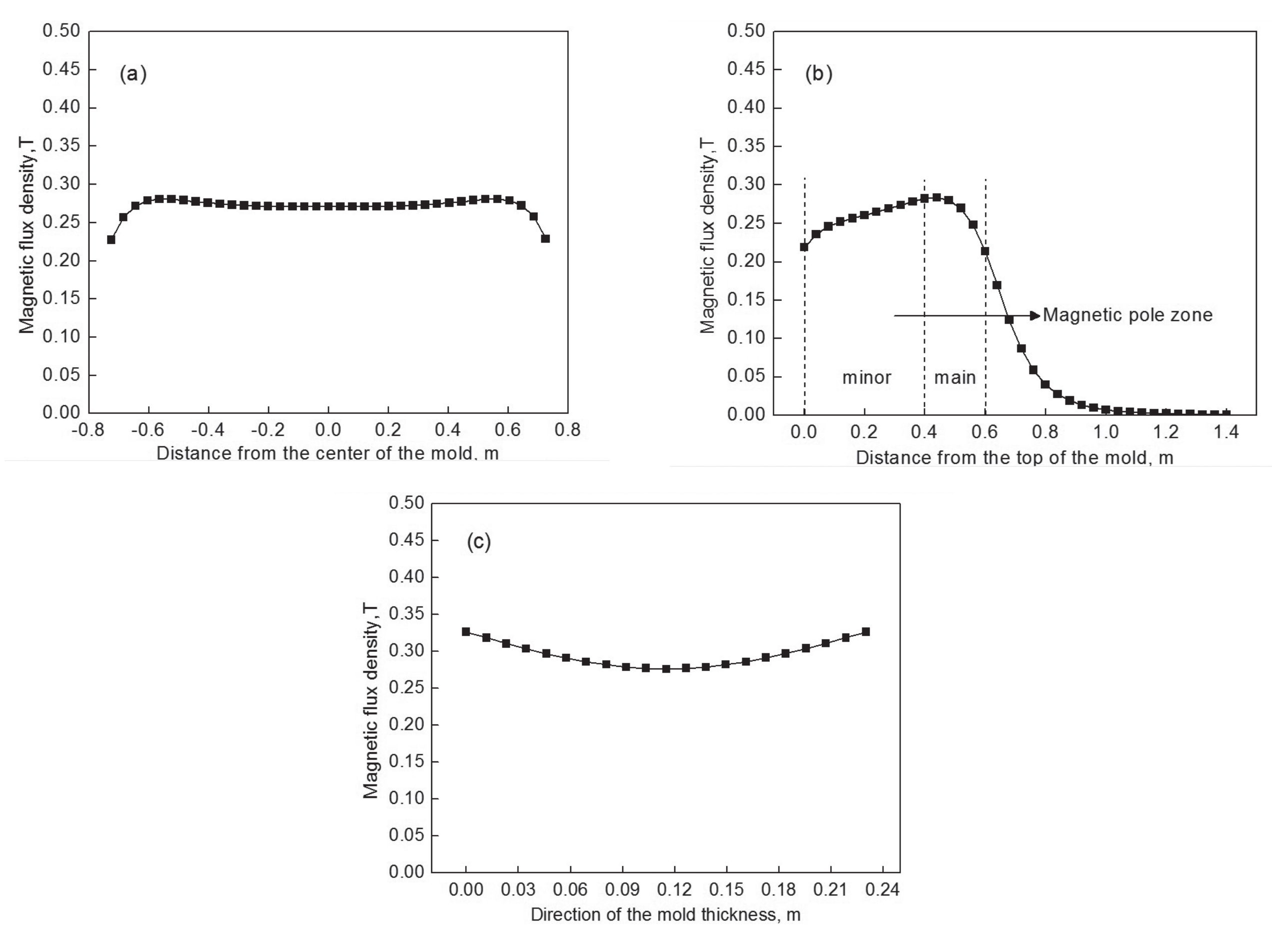

Fig. 3 - Distribution of magnetic flux density on linear VCW, VCH and VCT with VC-EMBr

(a) — VCW, (b) — VCH, (c) — VCT.

Fig. 3 shows that the trend of magnetic flux density on characteristic position is consistent with the result in Fig. 2. Along mold width direction (VCW), the distribution of magnetic flux density is relatively uniform, it is substantially the same except the left and right ends, and it is smaller at left and right ends since it is divergent at magnetic pole edges. Along mold height direction (VCH), the magnetic flux density is larger in the covered area of magnetic pole, from the lower edge to upper edge of main magnetic pole the magnetic flux density is increased gradually and the maximum value is at the upper edge, and then it is reduced gradually to the upper edge of minor magnetic pole, downward the lower edge of main magnetic pole it is decreased gradually. Along mold thickness direction (VCT), the distribution of magnetic flux density is an upward concave curve with very small gradient, the minimum magnetic flux density is at slab center and the maximum is at slab edge.

In summary, the design of the proposed new EMBr can form a stable magnetic field with sufficient strength in mold, and the effective magnetic flux density not only covers the entire mold width, but also covers the height range from free surface to the impacted point of molten steel jet near narrow face, when electric current is 850A, the maximum magnetic flux density in mold is about 0.36T. After applying the distribution of magnetic flux density of VC-EMBr with the above characteristics to continuous casting, the effect on molten steel flow in mold will be studied by numerical simulation results of flow field.

CALCULATED RESULTS AND ANALYSIS OF MOLTEN STEEL FLOW IN MOLD WITH VC-EMBr

Effect of VC-EMBr on Distribution of Flow Field in Mold

When the casting speed is 1.6m/min, the submerged depth of SEN is 170mm and outlet angle of SEN is -15°, the flow velocity vector in mold, flow velocity vector and turbulent kinetic energy contour of narrow face, flow velocity contour of free surface and flow velocity curves of free surface central line without and with VC-EMBr are shown in Fig. 4, Fig. 5, Fig. 6 and Fig. 7 respectively.

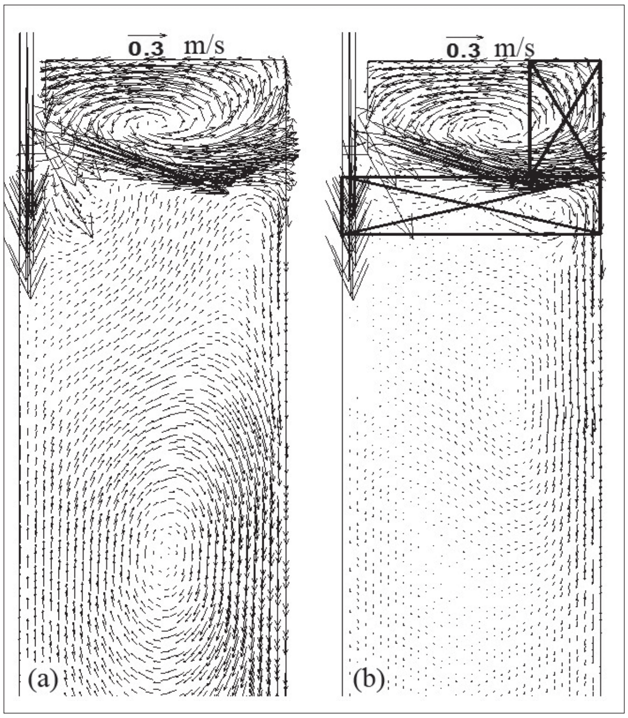

Fig. 4 - Flow velocity of molten steel in mold

(a) — No EMBr, (b) — VC-EMBr.

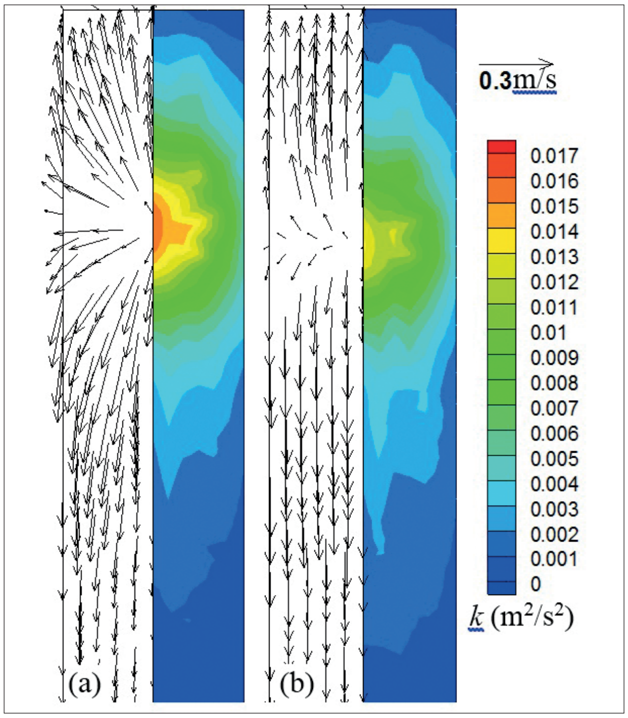

Fig. 5 - Flow velocity and turbulent kinetic energy of molten steel of narrow face

(a) — No EMBr, (b) — VC-EMBr.

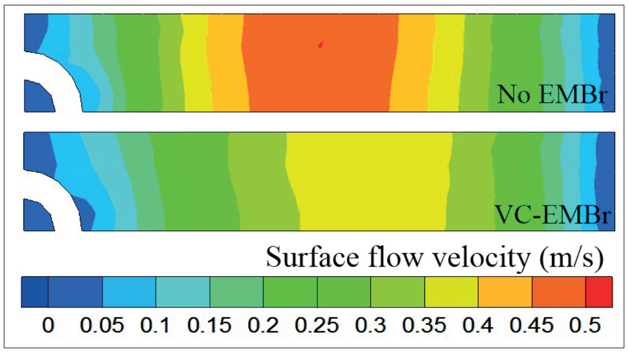

Fig. 6 - Flow velocity of molten steel of free surface in mold

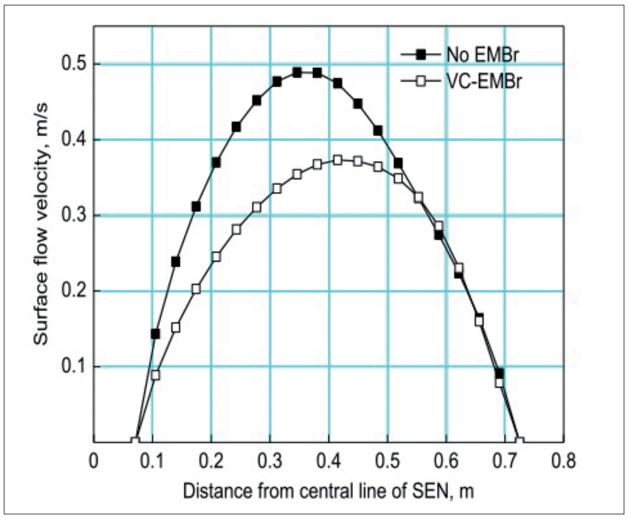

Fig. 7 - Flow velocity of molten steel of free surface central line

Comparing with the conventional continuous casting, the impacted strength of the molten steel jet from SEN on narrow face is decreased, the flow form of upper circulation is basically the same but flow velocity is reduced, the flow form of lower circulation is changed obviously and flow velocity is reduced significantly, the downward impacted depth of molten steel is reduced with VC-EMBr (Fig. 4). Flow velocity and turbulent kinetic energy of the impacted area on narrow face are decreased, the divergent degree of velocity distribution of the impacted point and its surrounding area is reduced significantly and the upward and downward flow around the impacted point on narrow face tend to regular flow distribution after applying VC-EMBr (Fig. 5). The flow velocity of free surface is decreased evidently, the maximum flow velocity of free surface central line is from 0.50m/s to 0.37m/s and the degree of decrease is 26% (Fig. 6, Fig. 7).

The numerical simulation results show that the steady DC magnetic field with electric current 850A of VC-EMBr can weaken the flow circulation in upper and lower mold significantly and inhibit velocity of the molten steel jet and its impacted strength on narrow face effectively. This can help to stabilize the surface fluctuations, reduce the slag, prevent leakage of molten steel and promote inclusion particles floating and separating, which illustrate that VC-EMBr can control the impact of the molten steel jet on narrow face while controlling the impacted depth in lower circulation and achieve the expected metallurgical effect.

Effect of VC-EMBr on Removal of Non-metallic Inclusion Particles in Molten Steel

The trajectories of inclusion particles can be obtained by tracking the positions of the particles in molten steel, the number of particles into free surface can be determined by the result of trajectories and thus the removal probability of inclusion particles is calculated. In this simulation, three groups of inclusion particles with different diameters are selected and there are 100 inclusion particles in each group for tracking, the first group is composed of 5μm, 20μm, 35μm and 50μm and each number is 25, the second and third group are composed of 100μm and 200μm respectively. When the casting speed is 1.6m/min, the submerged depth of SEN is 170mm and outlet angle of SEN is -15°, the trajectories of the three groups' inclusion particles without and with VC-EMBr are shown in Fig. 8 and Fig. 9.

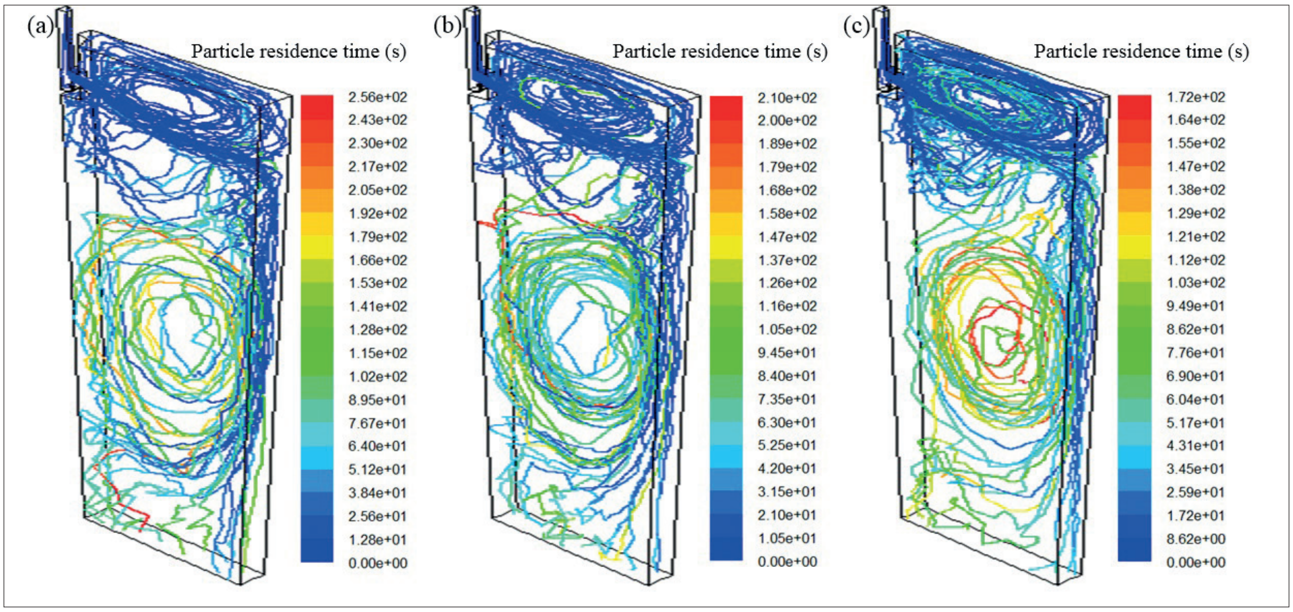

Fig. 8 - The trajectories of inclusion particles in mold without EMBr
(a) — 5μm to 50μm, (b) — 100μm, (c) — 200μm.

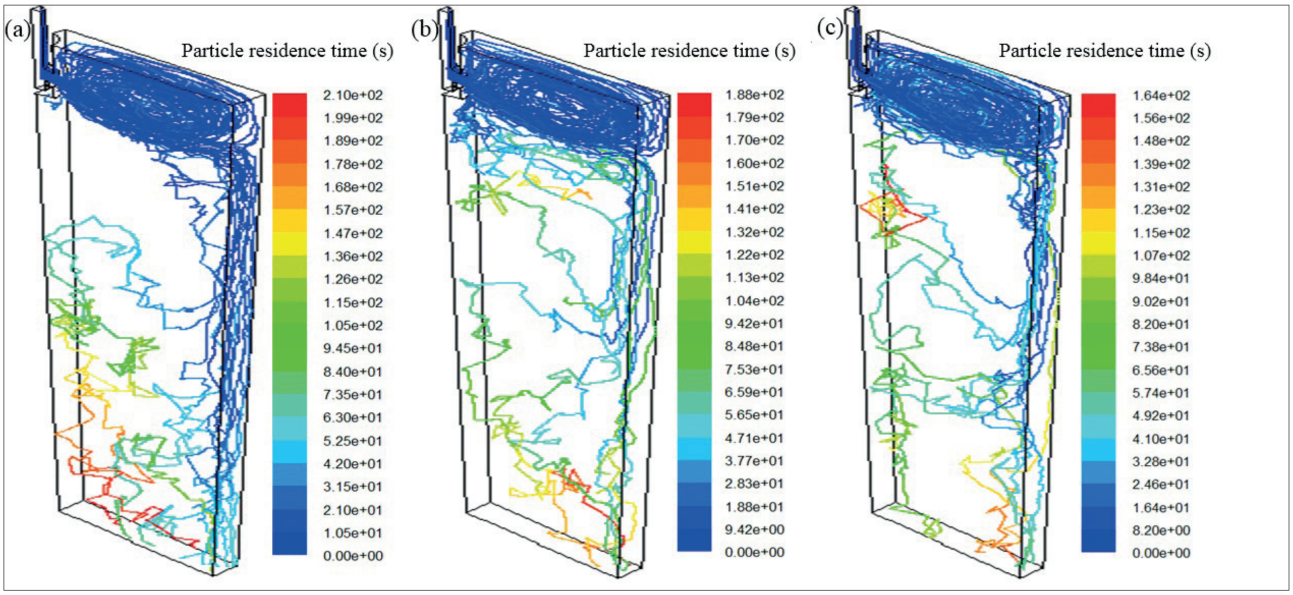

Fig. 9 - The trajectories of inclusion particles in mold with VC-EMBr
(a) — 5μm to 50μm, (b) — 100μm, (c) — 200μm.

Fig.8 shows that when EMBr is not applied, the result of tracking inclusion particles is similar to the distribution of flow field in mold, the inclusion particles which are ejected from SEN are divided into two parts, one part moves upward and the other moves downward, part of upward inclusion particles moving to free surface can be removed. After applying VC-EMBr, we can see that the upward portion of each group's inclusion particles is increased obviously and the downward portion is reduced significantly, the trajectories of inclusion particles in lower circulation is completely different from the previous and the particle residence time is reduced, so the number of inclusion particles floating to free surface will be increased, which illustrate that VC-EMBr can promote inclusion particles floating (Fig. 9). Moreover, the upward quantity of larger diameter particles is more than that of smaller diameter particles, so the floating number of larger diameter particles is more, and this is because the buoyancy of larger diameter particles is larger (Fig.8, Fig. 9).

For the number of inclusion particles moving to upper circulation is increased with VC-EMBr, the captured number of inclusion particles by free surface is bound to change. Make the removal number curves of inclusion particles with different diameters without and with VC-EMBr by the statistics, which are shown in Fig. 10.

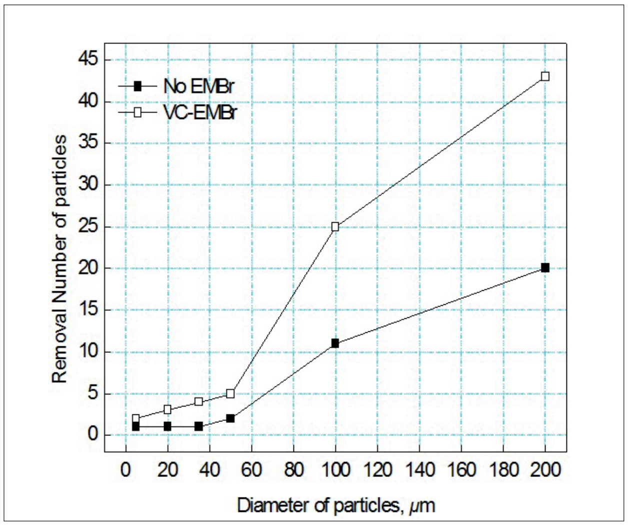

Fig.10 - The removal number of inclusion particles with different diameters

Fig.10 shows that when there is no EMBr, the removal number of inclusion particles with diameter 5μm, 20μm, 35μm and 50μm is 1, 1, 1 and 2 respectively, the removal number is 11 and 20 with diameter 100μm and 200μm respectively, so the removal probability of the three groups is 5%, 11% and 20%. After applying VC-EMBr, the removal number of inclusion particles with diameter 5μm, 20μm, 35μm and 50μm is 2, 3, 4 and 5 respectively, the removal number is 25 and 43 with diameter 100μm and 200μm respectively, the removal probability of the three groups is 14%, 25% and 43% respectively. So the removal probability of VC-EMBr is increased by 9%, 14% and 23% compared with conventional continuous casting.

The above numerical simulation results and statistical results illustrate that VC-EMBr has a significant effect on promoting inclusion particles floating and separating, the inclusion particles are more easily removed and the magnitude of removal effect on larger diameter (100μm, 200μm) is more obvious, which is beneficial to reduce the internal defect of slab and improve slab quality.

CONCLUSIONS

On the basis of V-EMBr, VC-EMBr technology which V-EMBr is combined with EMBr-Ruler is proposed, numerical simulation results show that it is possible to form an effective and sufficient strength magnetic field in mold, and the magnetic flux density not only covers the entire mold width, but also covers height scope from free surface to impacted point of molten steel jet near narrow face. The maximum magnetic flux density is approximately 0.36T with electric current 850A.

After applying VC-EMBr with electric current 850A, the numerical simulation results show that the molten steel jet from SEN is inhibited by electromagnetic force and impacted strength of it on narrow face is weakened, the molten steel velocity of free surface, molten steel velocity and turbulent kinetic energy of impacted point on narrow face are reduced, impacted depth in lower circulation and divergent degree of velocity distribution of narrow face are decreased significantly. The degree of decrease of surface flow velocity is about 26%, and the removal efficiency of inclusion particles with diameter 5μm to 50μm, 100μm and 200μm is increased by 9%, 14% and 23% than that of conventional continuous casting respectively. These phenomena indicate that VC-EMBr can control the narrow face area where the molten steel jet impacts while strengthening the control of impacted depth in lower circulation, and achieve to stabilize the surface fluctuations, reduce slag, prevent leakage of steel and promote inclusion particles floating and separating, which is conducive to reducing the surface and internal defects of slab and improving slab quality. The metallurgical effect of VC-EMBr is in line with the original design intent.

ACKNOWLEDGEMENT

This study was supported by the National Nature Science Foundation of China (No.51574083), the Program of Introducing Talents of Discipline to Universities (the 111 Project of China, No. B07015), the Program for Innovative Research Group of Liaoning Province' Universities (LT2010035) and Fundamental Research Funds for the Central Universities (No. N110609001).

REFERENCES

[1] K. Cukierski and B. G. Thomas: 'Flow control with local electromagnetic braking in continuous casting of steel slabs', Metall. Mater. Trans. B., 2008, 39, 94-107.

[2] H. Harada, E.Takeuchi, M. Zeze and T. Ishii: 'New sequential casting of different grade of steel with a level DC magnetic field', Testu-to-Hagane, 2000, 86, 278-284.

[3] A. Idogawa, M. Sugizawa, S. Takeuchi, K. Sorimachi and T. Fujii: 'Control of molten steel flow in continuous casting mold by two static magnetic fields imposed on whole width', Mater. Sci. Eng. A., 1993, 173, 293-297.

[4] C. Mapelli, A. Gruttadauria and M. Peroni: 'Application of electromagnetic stirring for the homogenization of aluminum billet cast in a semi-continuous machine', J. Mater. Process Tech., 2010, 210, 306-314.

[5] K. Timmel, S. Eckert and G. Gerbeth: 'Experimental investigation of the flow in a continuous-casting mold under the influence of a transverse, direct current magnetic field', Metall. Mater. Trans. B., 2011, 42, 68-79.

[6] R. Chaudhary, B. G. Thomas and S. P. Vanka: 'Effect of electromagnetic ruler braking (embr) on transient turbulent flow in continuous slab casting using large eddy simulations', Metall. Mater. Trans. B., 2012, 43, 532-553.

[7] R. Singh, B. G. Thomas and S. P. Vanka: 'Effects of a Magnetic Field on Turbulent Flow in the Mold Region of a

Steel Caster', Metall. Mater. Trans. B., 2013, 44, 1201-1221.
[8] K. Timmel, T. Wondrak, M. Röder, F. Stefani, S. Eckert and G. Gerbeth: 'Use of Cold Liquid Metal Models for Investigations of the Fluid Flow in the Continuous Casting Process', Steel Research Int., 2014, 85, 1283-1290.
[9] L. S. Zhang, X. F. Zhang, B. Wang, Q. Liu and Z. G. Hu: 'Numerical analysis of the influences of operational parameters on the braking effect of embr in a csp funnel-type mold', Metall. Mater. Trans. B., 2014, 45, 295-306.
[10] S.M. Cho, S. H. Kim and B. G. Thomas: 'Transient fluid flow during steady continuous casting of steel slabs: part ii. Effect of double-ruler electro-magnetic braking', ISIJ Int., 2014, 54, 855-864.
[11] K. Furumai, Y. Matsui, T. Murai and Y. Miki: 'Evaluation of defect distribution in continuously-cast slabs by using ultrasonic defect detection system and effect of electromagnetic brake on decreasing unbalanced flow in mold', ISIJ Int., 2015, 55, 2135-2141.
[12] F. Li, E. G. Wang, M. J. Feng and Z. Li: 'Simulation research of flow field in continuous casting mold with vertical electromagnetic brake', ISIJ Int., 2015, 55, 814-820.
[13] Y. H. Man, G. Hyun and H. S. Seung:' Numerical simulation of three-dimensional flow, heat transfer, and solidification of steel in continuous casting mold with electromagnetic brake', J. Mater. Process Tech., 2003, 133, 322-339.
[14] F. J. Wang: Computational Fluid Dynamics Analysis — Principles and Applications of CFD Software, Tsinghua University Press, Beijing, 2004, 132-145.
[15] B. E. Launder and D. E. Spalding: 'The numerical computations of turbulent flow', Comput. Method Appl. Mech. Eng., 1974, 3, 269-289.
[16] L. F. Zhang, S. B. Yang, K. K. Cai, J. Y. Li, X. G. Wan and B. G. Thomas:' Investigation of fluid flow and steel cleanliness in the continuous casting strand', Metall. Mater. Trans. B., 2007, 38, 63-83.